

Influence of landscape moisture sources and topography on rock weathering patterns associated with wildfire

Lisa Mol¹  | Michael Grenfell² 

¹Department of Geography and Environmental Management, University of the West of England, Bristol, UK

²Institute for Water Studies/Department of Earth Sciences, University of the Western Cape, Bellville, South Africa

Correspondence

Lisa Mol, Department of Geography and Environmental Management, University of the West of England, Bristol BS16 1QY, UK.

Email: lisa.mol@uwe.ac.uk

Funding information

The Bataleurs, Grant/Award Number: No award number - funding in kind (flight); British Society for Geomorphology, Grant/Award Number: ECR Research Grant 2015

Abstract

From 9 March 2015, a wildfire burned an area of 25.7 km², or approximately half of the Jonkershoek catchment (Western Cape, South Africa), over the course of 3 days. During this period, large areas of fynbos and commercial forest plantations were razed, and rocks, including boulders and smaller rocks, were exposed to high temperatures. While a substantial body of work has been carried out to investigate the effects of wildfire on landscape development, less is known about the effect of wildfire on rock weathering within a landscape. Previous studies have reported the overall effect of wildfire on rock deterioration, but the effect of intra-fire temperature differences associated with heat behaviour on a slope has not been sufficiently addressed. In this study we investigate the effects of topography and proximity to moisture on rock deterioration processes. In particular, we focus on the use of in-field rock deterioration measurements and GIS to investigate the relative influences of distance from burn source, distance from moisture source and topographical positioning of the sample site. The results indicate that boulder size and lithology are of secondary importance to the placement of fire-affected rocks within the wider topography of the landscape, and that rock exposure to moisture, also a function of landscape position, is likely to exacerbate the response of the rocks to heat. No direct correlation was observed between the type and severity of the outwardly visible damage sustained on the sampled rocks, and the size, lithology or proximity to burn source. We argue that these findings call for a re-evaluation of fire-related damage in the wider context of rock response as a function of topographical variations.

KEYWORDS

GIS, rock weathering, South Africa, topography, wildfire

1 | INTRODUCTION

Wildfires have become a routine feature in the newspapers in recent years, indicating an increase in their frequency as well as geographical distribution (Jolly et al., 2015). In particular, the summer of 2019 has set new records for high temperatures and wildfire occurrence across Europe, the USA and even the Arctic Circle, as reported in the media (see e.g. Solly, 2019). Moreover, current models suggest that wildfires are set to become more frequent as well as severe (Fairman et al., 2015; Potvin et al., 2016; Yue et al., 2015), as forest resilience to wildfires is lowering (Stevens-Rumann et al., 2018), which poses increasing risks to both ecological and human communities (Wigtill

et al., 2016). This anthropogenically driven shift in climate change-facilitated wildfires, in addition to factors such as increasing settlement and fire suppression (Abatzoglou & Williams, 2016; Kraaij & van Wilgen, 2014), therefore needs to be factored into the development of an increasing number of landscapes. In South Africa, in particular, changes in precipitation are unlikely to be uniform (Sian et al., 2021), and concerns have been raised about the projected rise in minimum temperature especially (Zhao et al., 2021).

Not only have weather patterns shifted to enhance drought conditions and high temperatures, thus priming the environment for elevated fire risk, but there is also mounting evidence that the changing types of vegetation are increasingly a fire fuel risk (Wotton

This is an open access article under the terms of the [Creative Commons Attribution](https://creativecommons.org/licenses/by/4.0/) License, which permits use, distribution and reproduction in any medium, provided the original work is properly cited.

© 2022 The Authors. *Earth Surface Processes and Landforms* published by John Wiley & Sons Ltd.

et al., 2017), which in turn shape the rate of energy release, flame characteristics, residence time and rate of spread of a fire (Sullivan et al., 2017, p. 51). Fuel aridity, which increases its susceptibility to ignition, has increased in line with drought and warming patterns (Abatzoglou & Williams, 2016). Revegetation, and in particular the growth of woody trees, has the ability to alter fire characteristics (occurrence and intensity) and is therefore of particular concern in areas which experience both droughts and tree regrowth (Collins et al., 2015). In South Africa, in particular, commercial forestry is often situated in erstwhile meadows or fynbos (Scott, 1993) next to existing woodland (Geldenhuys, 1997), which increases the fuel availability substantially. To add further risk, these plantations often consist of fast-growing species such as pine, which tend to burn with greater proportions of high-severity fire than slow-growth species such as redwood (Steel et al., 2015). In South Africa, in particular, the introduction of commercial forestry has enhanced the risk of high-intensity wildfires in areas where previously low-level vegetation with a lower fuel potential dominated (Scott, 1993). During drought conditions, these wildfires can pose a significant danger to wildlife and human population alike. This was particularly poignantly illustrated by the April 2021 wildfires in Cape Town, which led to the partial destruction of the campus of the University of Cape Town, including its historic Jagger library. Concerns have also been raised about the protection of older heritage, such as rock art, which can also be found in areas susceptible to wildfire. For example, Tratebas et al. (2004) showed that rock art is threatened not only by the appearance of large-scale spalls on rock art sites after a fire, but also by the adherence of ash deposit on these precious surfaces. This ash can persist well beyond the year the fire took place, when it is deposited within peels, flakes or spalls (Shtober-Zisu et al., 2018).

While some areas, such as savannahs, have developed to cope with frequent wildfire occurrence, and in fact thrive on it, there is increasing evidence that changes in wildfire occurrence frequency have a significant, and problematic, impact on the ecological system (Aponte et al., 2016). Chemical alterations to the soil, and associated loss of nutrients, are likely to affect recovery rates for the landscape (Jiang et al., 2016), increasing the long-term threat to ecosystem resilience in areas affected by an increasing frequency of wildfire. In upland areas, such as the research field site presented in this report, increased sediment runoff in the year following wildfire (Moody & Martin, 2001; Scott, 1993; Smith et al., 2011) and loss of fine topsoil material (Bormann et al., 2008) can lead to increased overland flow (Beeson et al., 2001), flash flooding and badland formation (Rulli & Rosso, 2007), which can be a further impediment to landscape recovery. Sass et al. (2012) observe a similar impact in the Tyrolean alps, where fire-affected slopes yielded roughly 10 times higher sediment volumes than undisturbed slopes. In this scenario the role of rock coverage can be crucial in protecting the surface when it is vulnerable to erosion, providing cover against direct precipitation impacts (Cerdà, 2001; Lavee & Poesen, 1991; Neave & Rayburg, 2007) and aeolian erosion (Guo et al., 2010; Li & Liu, 2003) in the absence of vegetation cover. The production of large spalls during fire events on large boulders and rocky outcrops can also alter the composition of the soil, resulting in increased stoniness (Shtober-Zisu & Wittenberg, 2021a) and likely lower erodibility of the surface. These studies indicate that rocks are likely to be subjected to deterioration processes associated with exposure to intense heat (see

Blackwelder, 1927; Emery, 1944; Ollier, 1983; Roth, 1975 for early work on this phenomenon). As Dragovich (1993) notes, rocks that are subjected to multiple wildfire events can exhibit a range of deterioration signals (e.g. spalling) associated with individual events, indicating a changing response depending on the wildfire conditions. Buckman et al. (2021) go as far as to suggest that fire damage to rocks can be a dominant driver of large landscape features such as flared slopes and inselbergs in semi-arid environments.

Some work has been carried out on the effect of fire on rock deterioration under controlled conditions; McCabe et al. (2007) simulated fire under controlled conditions and found that sandstone rocks exposed to fire deteriorated noticeably faster in comparison to similar rocks which had not been exposed to fire. This concurs with Goudie et al. (1992), who found that different lithologies subjected to fire under controlled conditions exhibited loss of elasticity at temperatures as low as 200°C, and Allison and Bristow (1999), who studied the effect of moisture (precipitation) on the response of rocks to wildfire. Other studies indicate that wildfire enhances rock deterioration rates in a natural setting, including the formation of micro-fractures on the surface (Dorn, 2003), and generally increases the rate of weathering (Bierman & Gillespie, 1991).

As shown in the preceding paragraphs, there is a large body of work on the occurrence of wildfire and its impact on landscape development. As Malkinson (2012) shows, wildfire behaviour is shaped by vegetation properties, weather patterns at the time of the fire and topography. However, these landscape-wide studies seldom take into account the small-scale topography of the affected area, such as hill-sides and small canyons, and the effect that this has on the distribution of temperatures and soot, in particular as controlling factors for rock deterioration, even though this has been shown to be a factor in the study of temperature distributions in tunnels (Hu et al., 2007; Li et al., 2012), tree trunks (Costa et al., 1991) and timber structures (Janssens, 2004). Fire requires fuel and oxygen to burn effectively, thus both the presence of fuel and air flow will alter the intensity with which a fire can burn. In natural settings, such as the one studied, the effect of the slope topography and its effect on air flow and fire propagation therefore needs to be considered. Previous research incorporating the effect of slope on wildfire propagation includes laboratory and computer simulations (see e.g. Sharples, 2008; Weise & Biging, 1997; Zhou et al., 2007), while investigations into geomorphic consequences of wildfire in natural settings are focused on the effects of the wildfire on the landscape (see e.g. Doerr et al., 2006; Pierson et al., 2001; Shakesby et al., 1993). The effect of landscape on wildfire propagation is acknowledged (see Sullivan, 2017 for an overview), as is the effect of topography on weather conditions that can exacerbate wildfire occurrence (Sharples, 2009), but this landscape-wide approach has not been incorporated in the assessment of rock weathering during a wildfire. When assessing the impact of wildfire on rock weathering, we need to consider that moisture gradients and fuel patterns change downslope (Bridge & Johnson, 2009), which will affect the moisture levels present in rock prior to the fire, as well as fuel availability in the vicinity of the rock. Rock weathering during a wildfire can thus be as much a function of the nature and condition of the rocks at the time of the fire as the positioning on the slope. In this study, these principles are extrapolated to the role topography plays in directing the intensity of the fire and the effect this has on the deterioration of rocks in the area. In this study, rock weathering

patterns are surveyed along three transects at different heights along a slope, and combined with topographic soil moisture analysis to investigate the effect that topography and moisture distributions have on the response of rocks to wildfire exposure.

2 | REGIONAL SETTING, SITE DESCRIPTION AND TRANSECT PLACEMENT

The Jonkershoek catchment is located near the town of Stellenbosch in the Western Cape (Figure 1). The general topographic structure of the catchment is characteristic of quartzitic sandstone Cape Fold Mountain terrain; strength-equilibrium rock slopes with variably thick, coarse debris footslope mantles, beneath steep cliffs (Boelhouwers & Meiklejohn, 2002; Moon, 1991). Catchment terrain is steep and highly dissected, with slopes of up to 77° (median = 18°). The mainstem valley is elongate in form, with the central axis oriented southeast (head) to northwest (outlet). Catchment lithology is illustrated in Figure 1a. The mountain toe-slope field site is underlain at depth by Stellenbosch Pluton granite of the Cape Granite Suite, with a surface cover

of Quaternary talus, gritty-sand and sandy soil. Soil thickness increases from <0.5 m through transect 1, to ~1.2 m through transect 3 (transect locations indicated in Figure 2). The surficial sparse debris of rock blocks that formed the focus of field measurements is derived from upslope outcrops of Peninsula Formation quartz arenite (Table Mountain Group; the mountain cap rock in Figure 1a) and Tygerberg Formation greywacke and quartz arenite (Malmsbury Group). Rock debris generation at present is considered to be driven by fire-induced spalling, sporadic seismic activity and sporadic frost wedging acting on a joint/fracture-induced secondary porosity (Boelhouwers, 1999), with the lattermost mechanism having been dominant during the cold-climate Pleistocene (Boelhouwers & Meiklejohn, 2002).

The zoomed-in frame in Figure 2 indicates that transects 1 to 3 are aligned down a hillslope profile from a near-crest position (T1), through the mid-slope (T2), to the footslope within the riparian margin of Tierkloof Stream (T3), and are thus aligned on a gradient from low to high long-term landscape moisture availability. This small hillslope profile is nested within the larger macro-scale mountain slope profile of sandstone cliffs, to debris-mantled footslopes, to the sparse debris-

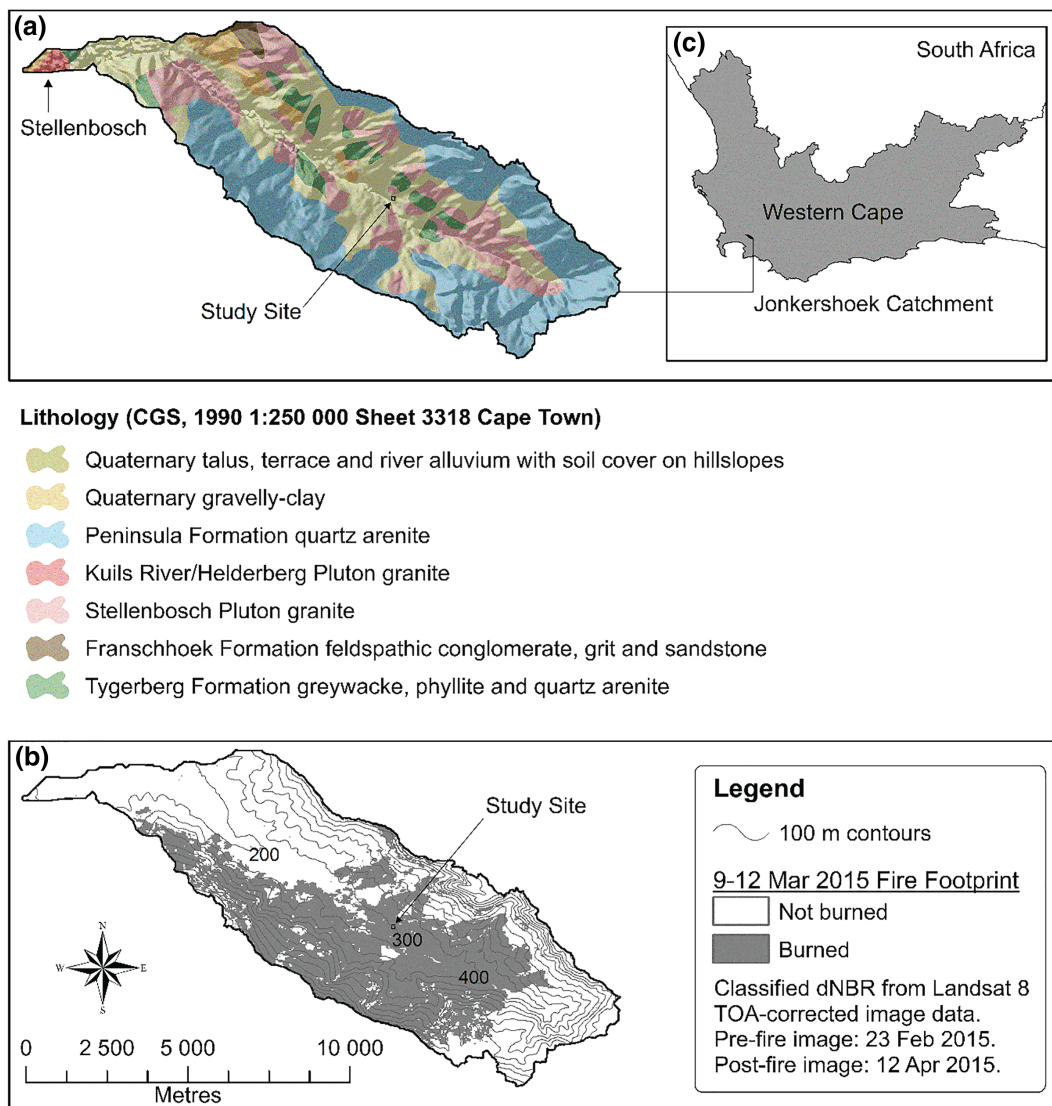


FIGURE 1 Location of the field site with respect to (a) lithology of the Jonkershoek catchment, Western Cape, South Africa and (b) burn footprint of the 9–12 March 2015 fire. The burn footprint was extracted using pixel threshold classification of a differenced normalized burn ratio (dNBR), as explained later in the text [Color figure can be viewed at [wileyonlinelibrary.com](https://onlinelibrary.wiley.com)]

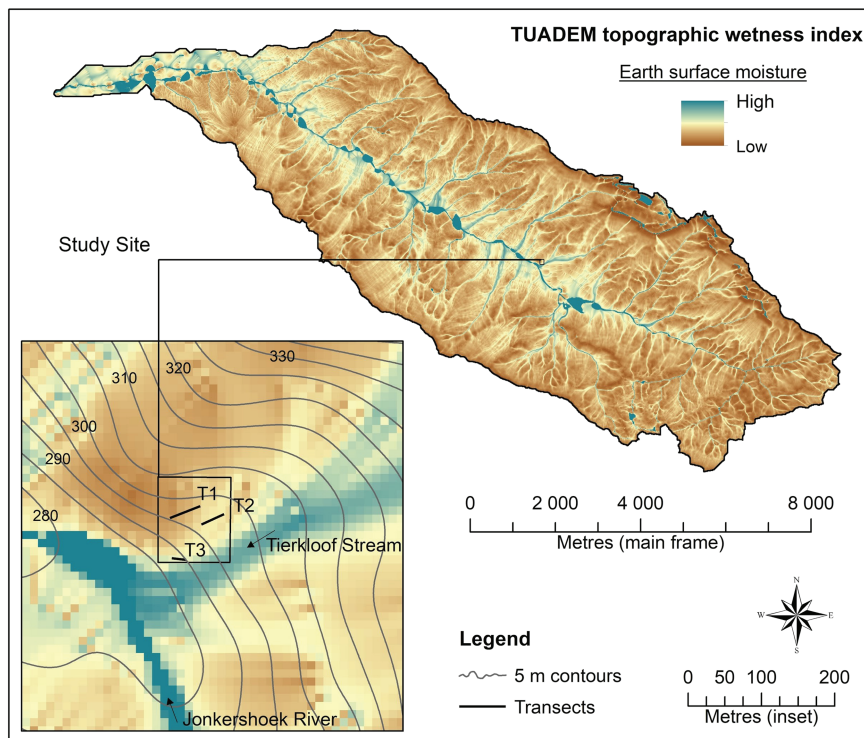


FIGURE 2 The study site in the context of potential landscape moisture variation, modelled by a topographic wetness index (TWI) [Color figure can be viewed at [wileyonlinelibrary.com](https://onlinelibrary.wiley.com/doi/10.1002/esp.5345)]

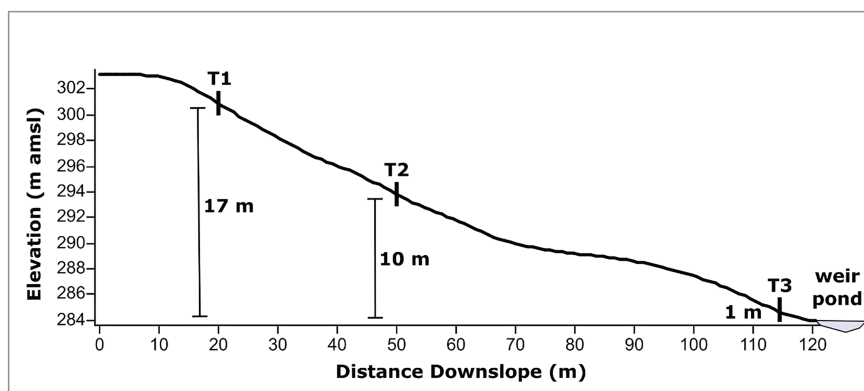


FIGURE 3 Relative height of transects, generated from a digital elevation model [Color figure can be viewed at [wileyonlinelibrary.com](https://onlinelibrary.wiley.com/doi/10.1002/esp.5345)]

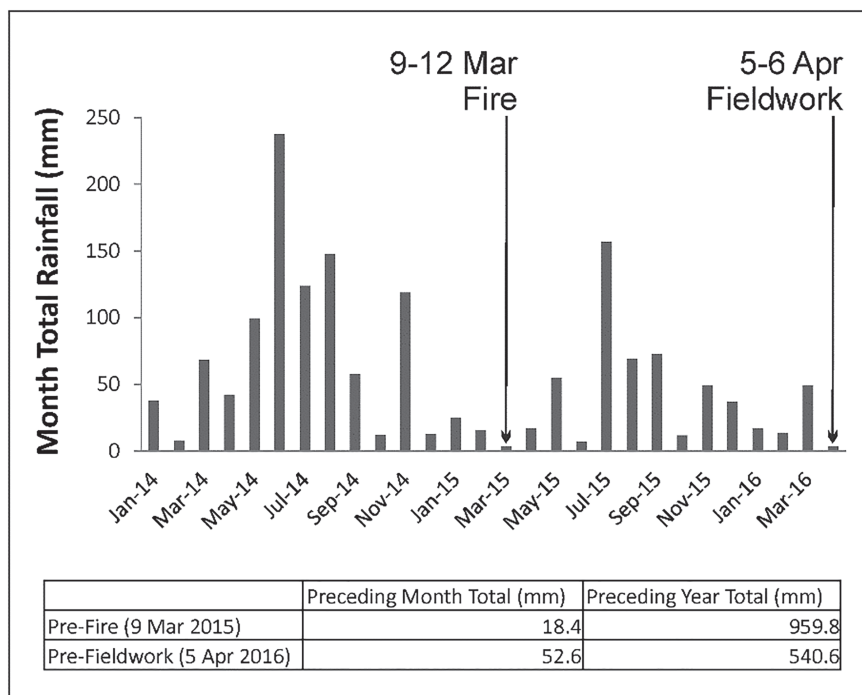
covered dissected toe-slope on which the study site is located. Top-down parent material supply by the sandstone cliffs to the mountain toe-slope weathering system is thus mediated by the macro-scale mountain slope system, while local moisture variation is mediated by the site-scale hillslope system (Figure 2). The placements of the transects are further illustrated in Figure 3, showing the cross-section of transects at their relative heights on the slope.

The field site falls within Vegetation Unit FFg2, Boland Granite Fynbos (nomenclature after Rebelo et al., 2006). General climate characteristics associated with this vegetation type are a mean annual precipitation (MAP) of 610–2220 mm, a range in daily mean temperatures of 5.9°C (July) to 26.6°C (February) and a typical frost incidence of 2–3 days per year (Rebelo et al., 2006). The gauged record for Jonkershoek indicates a catchment-wide MAP of 1390 mm (Moses, 2008). Northwesterly-driven winter rainfall dominates, although summer rainfall does occur as local up-valley pressure gradient winds interact with the near-vertical valley head (Moses, 2008). MAP varies markedly with elevation (Moses, 2008), and is about 900 mm at the elevation of the field site (Maswanganye, 2017). MAP

varies slightly with aspect, with the northwest-facing valley head area receiving highest rainfall, and west-facing slopes receiving about 100 mm more MAP than east-facing slopes (Maswanganye, 2017). The field site is located on a southeast-facing slope of a tributary sub-catchment (Tierkloof), which is nested within the low-insolation southwest-facing flank of the larger Jonkershoek catchment (Figure 2). The site received close to the long-term annual average rainfall over the year preceding the fire, but only received about half that figure in the year between the fire and the fieldwork campaign (Figure 4), which signalled the start of the prolonged and much publicized Cape Town drought. An overall reduction in frontal rainfall is expected in future due to the poleward expansion of the South Atlantic anticyclone (Jury, 2019), thus increasing the likeliness of year-on-year increases in drought occurrence and enhanced wildfire risk.

The dominant vegetation species at the site and time of field survey along transect 1 included grasses such as *Aristida congesta* and *Briza minor*, fine-stemmed restios such as *Restio debilis* and *Restio egregius* and bulbs that were not flowering at the time of survey. transect 2 was dominated by the shrubs *Salvia chamelaeagnea*, *Halleria*

FIGURE 4 Rainfall totals and monthly pattern over the year preceding the fire, and the year between the fire and the field campaign. Such variation would make direct surface moisture measurements taken at the time of the field campaign unrepresentative of the longer-term landscape moisture variation, illustrating the need for insight derived from the TWI



elliptica and *Asparagus rubicundus*, and the same grass species as transect 1. Burned stumps and some remaining charred stems of *Pinus radiata* (part of the Jonkershoek commercial plantation) were present in the area covered by transects 1 and 2, with individual stumps spaced about 3 m apart. Transect 3 within the riparian margin was dominated by large individuals (and large charred stumps) and saplings (some charred) of the indigenous Rooiels tree *Cunonia capensis*, with a ground cover of small shrubs such as *Asparagus scandens*. Figure 5 shows the transects within their post-fire vegetative settings.

The fires that prompted the current study started on 9 March 2015 and had been largely contained by 12 March 2015. The extent of the burned area indicated in Figure 1b is 25.7 km², which amounts to 43% of the overall 59.3 km² Jonkershoek catchment area. As an indicator of fire severity, *Pinus radiata* stumps in the vicinity of transects 1 and 2 had a diameter of 100–150 mm, and would have dominated the fuel load in this area, especially given that the indigenous shrubs (5–20 mm stem diameter), restios (1–3 mm stem diameter) and grasses (1 mm stem diameter) present during our post-fire survey would likely have been suppressed by the canopy cover of the pine plantation. Stumps of the indigenous tree *Cunonia capensis* along transect 3 had a diameter of 200–400 mm and would have dominated the fuel load in this area. It should be noted that fire is a natural and necessary component of fynbos ecology, with the lifecycle of many fynbos species set to the natural fire return period, which can vary from 10 to 40 years depending on location (Kraaij & van Wilgen, 2014; van Wilgen et al., 2010). The Jonkershoek catchment lies close to the divide between the ‘Western inland’ and ‘Western coastal’ fire climate zones, with fire return intervals of 12 and 14 years, respectively (Kraaij & van Wilgen, 2014). More frequent fire ignition by accident and arson is becoming a concern within the Cape Floristic Kingdom (Kraaij & van Wilgen, 2014), and is particularly problematic in areas under commercial plantation forestry with unnaturally elevated fuel loads (van Wilgen et al., 2010). Parts of the Jonkershoek catchment had burned prior to 2015 as recently as 2009, and the entire

catchment burned again in 2020 (i.e. approximately half the expected fire return interval time for this region; Kraaij & van Wilgen, 2014).

3 | METHODS

3.1 | Landscape physiographic analysis

The burn footprint of the 9–12 March 2015 fires (Figure 1b) was derived using Jenks classification of a Landsat8 TOA-corrected differenced normalized burn ratio (dNBR), which is the map algebra difference of pre- and post-fire NBR products (see Escuin et al., 2008). The NBR discriminates between vegetation and bare ground through differences in near-infrared and short-wave infrared reflectance. Pre/post-fire differencing was necessary to prevent misclassification of unvegetated rock surfaces (which are common in the catchment) as burned area.

A topographic wetness index (TWI) for the entire catchment (Figure 2) was derived from a 5 m-resolution void-filled digital terrain model using TAUDDEM (Tarboton, 1997). High TWI values indicate areas of high flow accumulation (D_{∞} flow routing) and low slope, which would typically be associated with high earth surface moisture availability (e.g. Leh et al., 2008). Since slope length (and thus specific catchment area, or flow accumulation) increases, and slope steepness decreases, from near the hill crest at transect 1 to the hill base within the riparian zone at transect 3, one would expect long-term average moisture conditions in the near-surface soil and rock-cover environment to increase in a downslope direction, with implications for pre-fire rock-cover moisture exposure.

3.2 | Rock weathering surveys

Semi-quantitative rock weathering surveys were carried out using the following variables, with associated hypotheses as shown in Table 1.



FIGURE 5 Overview photos of the transects, showing the sampled rocks and their setting within the vegetation [Color figure can be viewed at [wileyonlinelibrary.com](https://onlinelibrary.wiley.com/terms-and-conditions)]

Each variable was assigned a sliding scale of 0 (not present) to 5 (dominant), as adapted from previous rock weathering studies (see e.g. Cerveney et al., 2016; De Vente & Poesen, 2005; Dorn et al., 2012). While this is a semi-quantitative undertaking, the surveys were carried out by one researcher, thus reducing user variability that could affect the consistency of the assessments. Table 2 shows the scale used for each fire damage variable.

In addition, the geographical location of each sample rock was noted as well as the size of each sample rock. The width of the rock was defined as the measurement in centimetres perpendicular to the slope, whereas the length was defined as the measurement in centimetres parallel to the slope.

3.3 | Rock surface hardness measurements

As several studies have demonstrated (see e.g. Aoki & Matsukura, 2007; Betts & Latta, 2000; McCarroll, 1991; Mol &

Viles, 2012), rock surface hardness can be used as a key indicator of the degree of weathering of a surface. To quantify rock surface hardness, an Equotip 3 with D-type probe was used to map differences in hardness of the sample rock surfaces. This equipment was originally developed for the testing of metals (Viles et al., 2011), but is now used in both natural settings (Coombes et al., 2013; Pérez Alberti et al., 2013) and the built environment (Wilhelm et al., 2016). The surface hardness is measured through rebound of a 3 mm-diameter spherical tungsten carbide test tip against the rock surface. This tip is mounted in an impact body and impacts under spring force against the test surface from which it rebounds (Verwaal & Mulder, 1993). The velocity before impact (V_1) and after impact (V_2) are measured automatically and displayed as a ratio ($V_2/V_1 \times 1000$), which is denoted by the unit 'L', or Leeb unit (Hack et al., 1993).

Repeated rebound of the impact device against the surface can result in an artificial increase in measured strength due to compaction of the surface (Hansen et al., 2013). To minimize this effect and avoid artificial compaction of the surface, 30 measurements were taken within a 10×10 cm space, but never on the exact same position, after manually cleaning the surface of debris such as mud and grit. This test was repeated on each distinctive surface of the sample rocks (e.g. surface with a distinct soot layer, as well as freshly exposed surfaces where sample rocks had split) to map variability in rock surface hardness. In total, 47 surfaces were measured. By calculating both the mean value per section measured and the standard deviation, the weathering progression was estimated at all test sites.

4 | RESULTS

4.1 | Topographic wetness index

To estimate the exposure of the sampled sites to moisture, TWI values were compared for the three transects. Normalized (0–1) TWI values extracted from the raster model (Figure 2) indicate a systematic increase in long-term average surface moisture availability from transect 1 to 3 (in the downslope direction). The transect-average normalized TWI for transect 1 (beneath rock samples 1 to 16) is 0.171 (6 pixels), for transect 2 (beneath rock samples 17 to 33) it is 0.232 (6 pixels) and for transect 3 (beneath rock samples 34 to 43) it is 0.285 (4 pixels). Pixel-based normalized TWI data are summarized in Table 3. For landscape-scale reference, normalized TWI values approaching or reaching 1 occur in low-slope reaches of the mainstem Jonkershoek River that are near-permanently inundated by shallow flow, whereas normalized TWI values of 0.45–0.6 are typical within the local Tierkloof Stream thalweg adjacent to the study site.

These data indicate that the rocks situated at the bottom of the slope (T3) are likely to be exposed to higher moisture levels throughout the year, thus facilitating capillary flow into the rock and higher sustained internal moisture levels. In contrast, the rocks situated at the top of the slope (T1) are likely to experience very low exposure to capillary rise of moisture. While the effect of higher moisture content in sedimentary rock as an agent of deterioration during a fire has not previously been conclusively researched, it has been shown that water is up to 23 times more efficient in transferring heat than air (Denny, 1993 p. 147). This is confirmed by Deal (2012), who suggests that higher moisture content can lead to increased transfer of heat in

TABLE 1 Hypotheses used for the semi-quantitative rock weathering survey and their wider literature base

Variable	Hypothesis	Supporting literature
Sample rock size	(1) Larger rocks are relatively less affected by fire damage than smaller rocks	Disputed by Dorn (2003) Shtober-Zisu and Wittenberg (2021b)
Distance to nearest burn source	(2) The closer a rock is situated to a burn source, the more intense the damage from the fire will be across all measured variables	Escuin et al. (2008) Gunn (2011) Pozo-Antonio et al. (2020)
Quartz content of the sample rock	(3) Penetration depth of heat and the associated damage types vary as a function of lithology	Sippel et al. (2007)
Colour difference surface vs. interior of rock	(4) Iron oxidation and mobilization will be visible in rocks affected by heat	McCabe et al. (2007) Hajpál and Török (2004) Kompaníková et al. (2014) Gillhuber et al. (2010)
Soot deposition/black crust formation	(5) The closer a rock is situated to a burn source, the thicker the soot deposit will be	Bierman and Gillespie (1991)
Appearance of cracks (macro >1 mm and micro <1 mm)	(6) Newly formed cracks, as evidenced by a freshly exposed surface, are associated with fire damage	Allison and Bristow (1999) Goudie et al. (1992) Jackson (1998)

TABLE 2 Overview of the variables investigated and the sliding scale used for identification of the damage intensity. Note that all observations were carried out by one researcher to minimize inconsistency in the interpretation of damage intensity and associated semi-quantification

Variable	Sliding scale
Quartz content of the sample rock	0 = no quartz crystals observed; 1 = observed quartz content 10–20% of visible matrix; 2 = observed quartz content 20–40% of visible matrix; 3 = observed quartz content 40–60% of visible matrix; 4 = observed quartz content 60–80% of visible matrix; 5 = observed quartz content 80–100% of visible matrix
Colour difference surface vs. interior of rock	0 = no discernible difference; 1 = light discolouration to very light pink; 5 = discolouration from light grey or white to dark red
Soot deposition/black crust formation	0 = no visible soot; 2 = <25% of surface covered; 3 = <50% of surface covered; 4 = <75% of surface covered; 5 = wholly covered in soot, no original surface visible
Appearance of cracks (macro >1 mm and micro <1 mm)	0 = no visible surface cracks; 1 = some very small cracks visible (<1 cm in length); 2 = some small cracks visible (<5 cm in length); 3 = incidental cracks present across the whole surface; 4 = cracks visible across the whole surface, forming a network; 5 = structural stability of the surface compromised by comprehensive cracking of the surface

obsidian during a fire event. In the longer term, Gomez-Heras et al. (2009) show that fire-related damage, such as cracking, can be further exploited by moisture and lead to enhanced deterioration rates. It is therefore likely that in the event of repeated wildfires in an area, as has been observed at the study site, not only is heat transfer in the rocks likely to be greater in those exposed to soil moisture, but these rocks can also be subject to enhanced deterioration in the periods between wildfires.

4.2 | Rock samples size and lithology distribution

To test the relative influence of rock sample size on fire response (hypothesis 1), the width and length of each sample was measured. The length was taken as the longest possible measurement across the sample parallel to the slope, and the width as the longest possible measurement perpendicular to the slope. As shown in Figure 6, the maximum length and width of the samples were roughly equal across the majority of samples, but rock sample size varied across the transects with the majority of larger samples. As expected, some gravitational sorting had taken place, where the largest boulders were found at the bottom of the slope (T3), while the transect in the middle of the slope showed relatively small samples (T2) and the transect on top of the slope had retained a few larger samples (T1), as shown in Figure 6. This is in line with gravitational sorting of boulders on slopes connected to rock fall from surrounding cliff faces, as reported by Haas et al. (2012).

Three types of sandstone were identified using a hand lens (Figure 7): (1) Peninsula Formation light grey quartz arenite, Table Mountain Group (Ordovician Cape Supergroup); (2) Tygerberg Formation quartz arenite (Malmesbury Group); and (3) Tygerberg Formation greywacke (Malmesbury Group) (refer to Figure 1a for the spatial distribution of outcrops upslope of the field site). Although phyllite is represented within the Tygerberg Formation, there was no evidence of this material surviving on any of the three transects.

The majority of the rocks identified are Tygerberg Formation quartzitic sandstone ($N = 29$, 67%), followed by Peninsula Formation quartzitic sandstone ($N = 10$, 23%) and Tygerberg Formation

TABLE 3 Normalized (0–1) TWI pixel values along transects 1 to 3, extracted from the raster model shown in Figure 2

	Distance along transect covered by pixel (m)	Pixel normalized (0–1) TWI value
Transect 1	0–5	0.194
	5–10	0.197
	10–15	0.172
	15–20	0.159
	20–25	0.164
	25–30	0.140
	Mean	0.171
	StDev	0.022
Transect 2	0–5	0.239
	5–10	0.231
	10–15	0.238
	15–20	0.229
	20–25	0.236
	25–30	0.219
	Mean	0.232
	StDev	0.007
Transect 3	0–5	0.305
	5–10	0.279
	10–15	0.276
	15–20	0.278
	Mean	0.285
	StDev	0.014

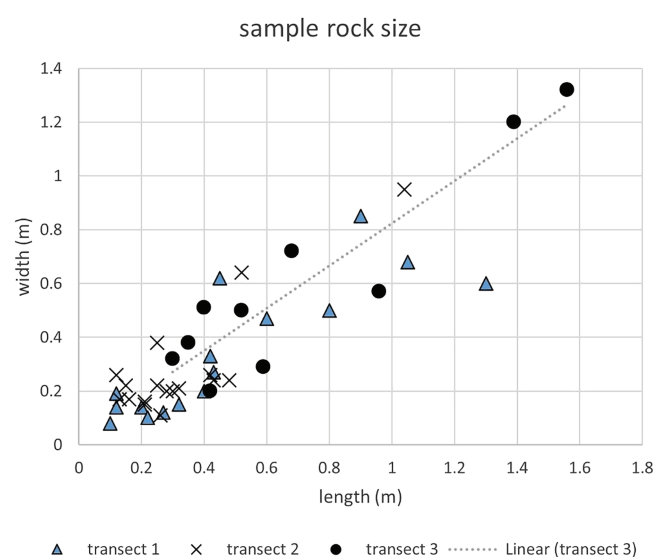


FIGURE 6 Size distribution of rock samples across all three transects, showing a clustering of smaller samples along transect 2, whereas larger samples are predominantly found along transect 3. Transect 1, at the top of the slope, covers a larger variety of rock samples [Color figure can be viewed at [wileyonlinelibrary.com](https://onlinelibrary.wiley.com)]

greywacke ($N = 4$, 10%). The Peninsula Formation sandstone appears to be the most resistant to weathering processes out of all measured rocks, recording both the largest average sample size and surface hardness (see Table 4).

At a transect-wide scale, there is weak evidence that the harder rock samples (e.g. the Peninsula Formation quartzitic sandstone, Leeb hardness > 500) exhibit higher standard deviations, which in the study by Rodríguez-Rellán (2016) is associated with larger discontinuities such as cracking and flaking of the surface. As Figure 8 illustrates, this is particularly prevalent on transect 3, where the majority of the Peninsula Formation samples are located. On transect 2 there is a weak correlation between higher than average hardness values and higher standard deviation values. The standard deviation on transect 1 is highly variable, and shows little correlation between hardness values recorded per sample and associated standard deviations.

4.3 | Damage susceptibility as a function of distance to burn source (hypothesis 2)

As shown in Figure 9, no statistically viable correlation was found between the distance between the nearest burn source, indicated by tree and shrub stumps, and the intensity of the damage to the rocks (hypothesis 2). The most viable relationship ($R^2 = 0.3362$) was found between the distance to the burn source and the blackening of the surface on transect 1 (top of the slope). Here, the sample rocks closer to the burn source were slightly more likely to develop a noticeable black crust, which is likely to be related to soot particles airborne in the immediate area of high temperature around the burn source. This is consistent with the idea of a buoyant plume above the burn source (Zang & Li, 2017), where high temperatures within the valley facilitate the rapid rise of air, thus entraining soot particles into the atmosphere, with subsequent deposition when this heated air mixes with slightly cooler air on top of the slopes. These particles are then deposited when air temperatures drop further away from the burn source. However, these temperature gradients will vary according to type and availability of fuel, thus accounting for the weak statistical relationship.

4.4 | Damage susceptibility as a function of rock sample size (hypothesis 1) and type (hypothesis 3)

As Figure 10 indicates, no viable relationship was found between the total deterioration score (discolouration, cracking, flaking, crumbling) and rock sample size. However, when power functions were fitted to the clusters of transect measurements, the overall damage scores for transect 3 are on average higher than those of transects 1 and 2. Damage scores of transect 2 were overall the lowest, as indicated by the power function line.

Across the identified lithologies, there is very little difference in the average damage scores recorded; Malmsbury greywacke samples recorded on average 11.5 damage points, Malmsbury sandstone a total average of 12.0 and Peninsula sandstone 10.8 damage points on average. There does not appear to be a statistically viable

FIGURE 7 Size distribution of the identified lithologies [Color figure can be viewed at wileyonlinelibrary.com]

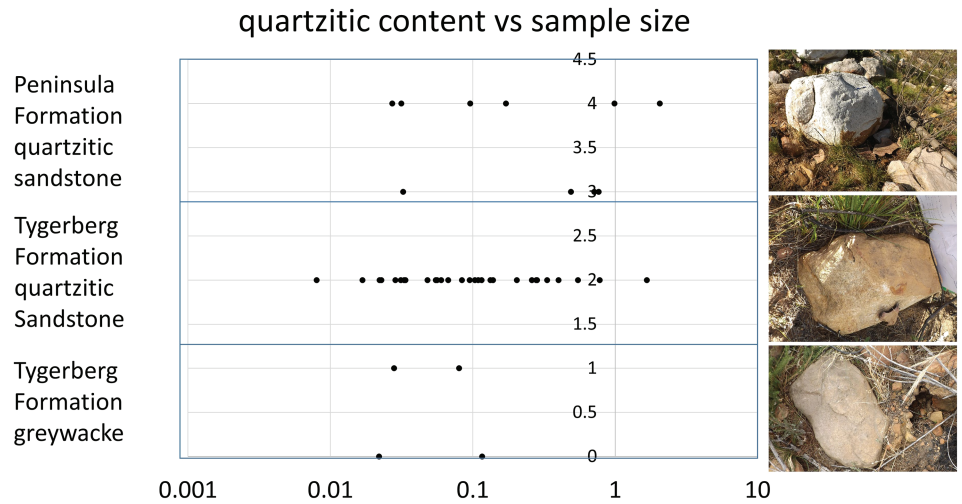


TABLE 4 Sample classification, size and surface hardness results

Rock classification	N	Average size	Standard deviation	Average Leeb hardness	Standard deviation
Peninsula Formation quartzitic sandstone	10	0.368 m ³	0.609	573.13	54.44
Tygerberg Formation quartzitic sandstone	29	0.155 m ³	0.326	476.86	69.98
Tygerberg Formation greywacke	4	0.062 m ³	0.039	453	114.86

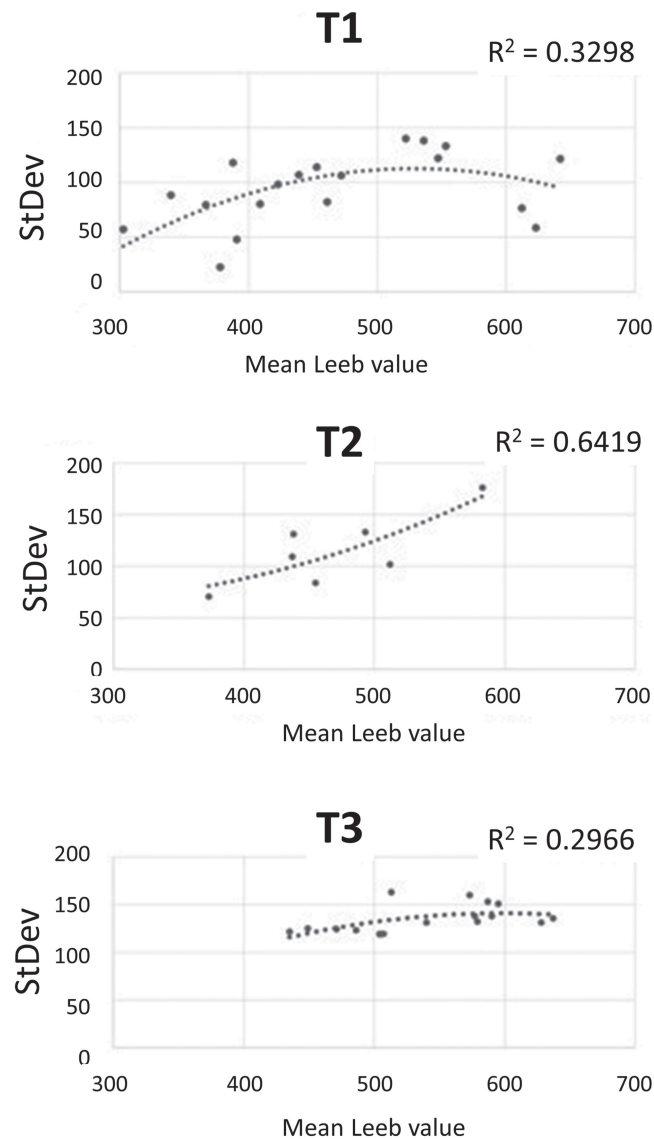


FIGURE 8 Mean Leeb values for all measured rock samples, split out according to transect

relationship between the damage incurred by wildfire and the type of lithology.

4.5 | Internal (hypothesis 4) and external (hypothesis 5) discolouration of sample rocks

To assess the spatial variation of discolouration, the data are analysed here per transect to investigate spatial deposition patterns. Black discolouration refers to the deposition of soot on the surface of the sample rock, leading to a black carbon crust. This soot is associated with incomplete combustion of particles, away from the direct fire where the temperatures are lower (Obaidullah et al., 2012). In contrast, red discolouration of the rock is associated with high temperatures found within reach of the flames (Gomez-Heras et al., 2009), as the transition from the beige colour of the sandstone to light red/orange, and dark red which is associated with temperatures above 400°C (Kompaníková et al., 2014).

As Figure 11a shows, the majority of soot deposition is confined to transects 1 and 3. For transect 3 this is likely connected to incomplete combustion of the vegetation at the bottom of the slope, associated with lower temperatures and ‘greener’ fuel (for the case of the indigenous Rooiels trees, relative to the planted pines higher up the slope). In the case of transect 1, further deposition of the soot has taken place at the top of the slope, where the partially combusted particles carried in the hot air are deposited. It is likely that this happens as the buoyant plume meets the slightly cooler air above the slope, loses the energy required to keep the soot particles buoyant and deposits them on top of the slope (in this case on the surfaces of the measured rock samples on transect 1).

Dark red discolouration is most profound at transects 1 and 3 (Figure 11b), where the heat is likely to have been most intense (Mordandini et al., 2001), and less profound at transect 2, where both smaller fuel sources were available and the hot air generated by the fires rises rapidly to the top of the slope. Light red discolouration,

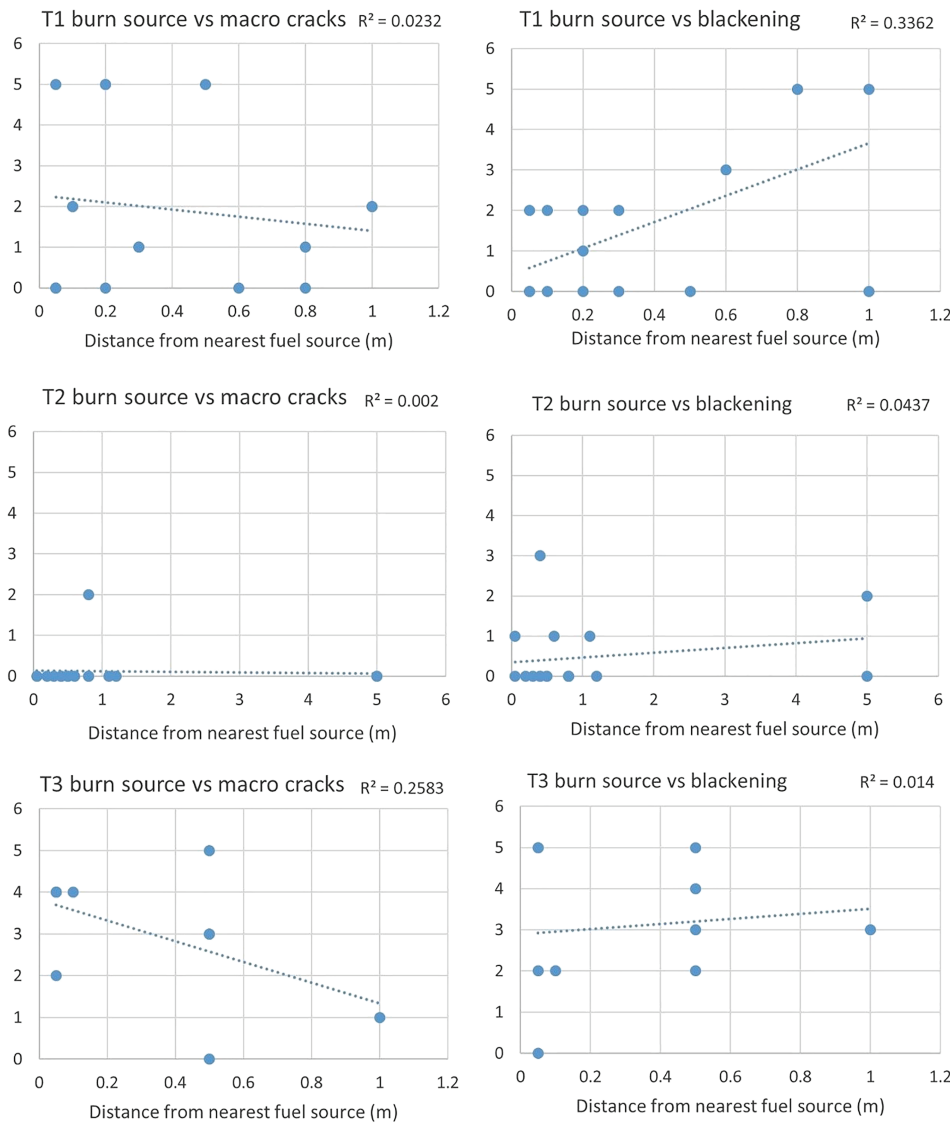


FIGURE 9 Relationships between damage type and distance from nearest fuel source. These graphs show that no clear correlations were found between the distance to the burn source and cracking and blackening intensity [Color figure can be viewed at wileyonlinelibrary.com]

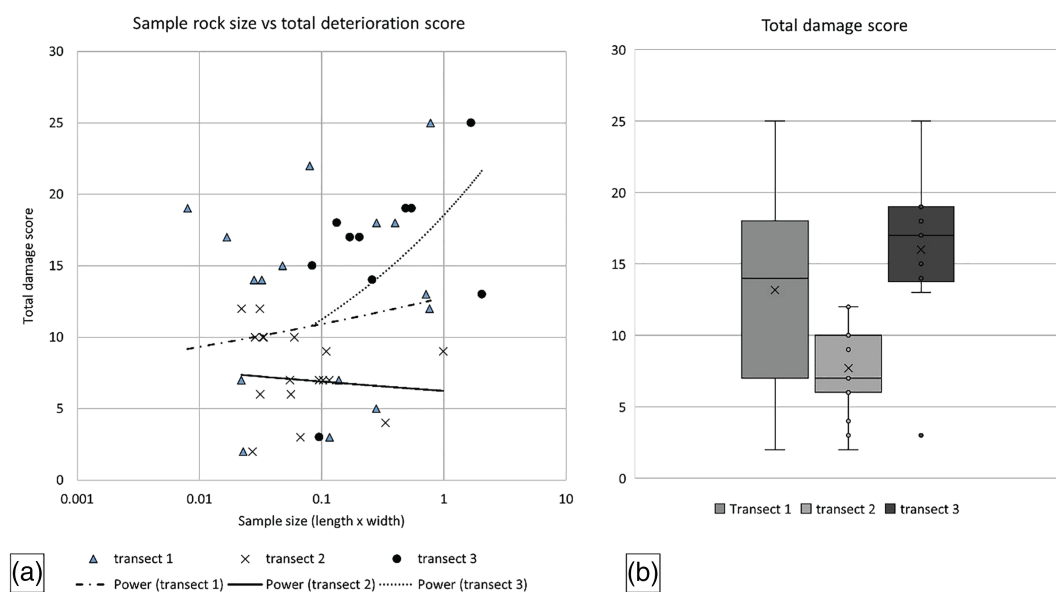
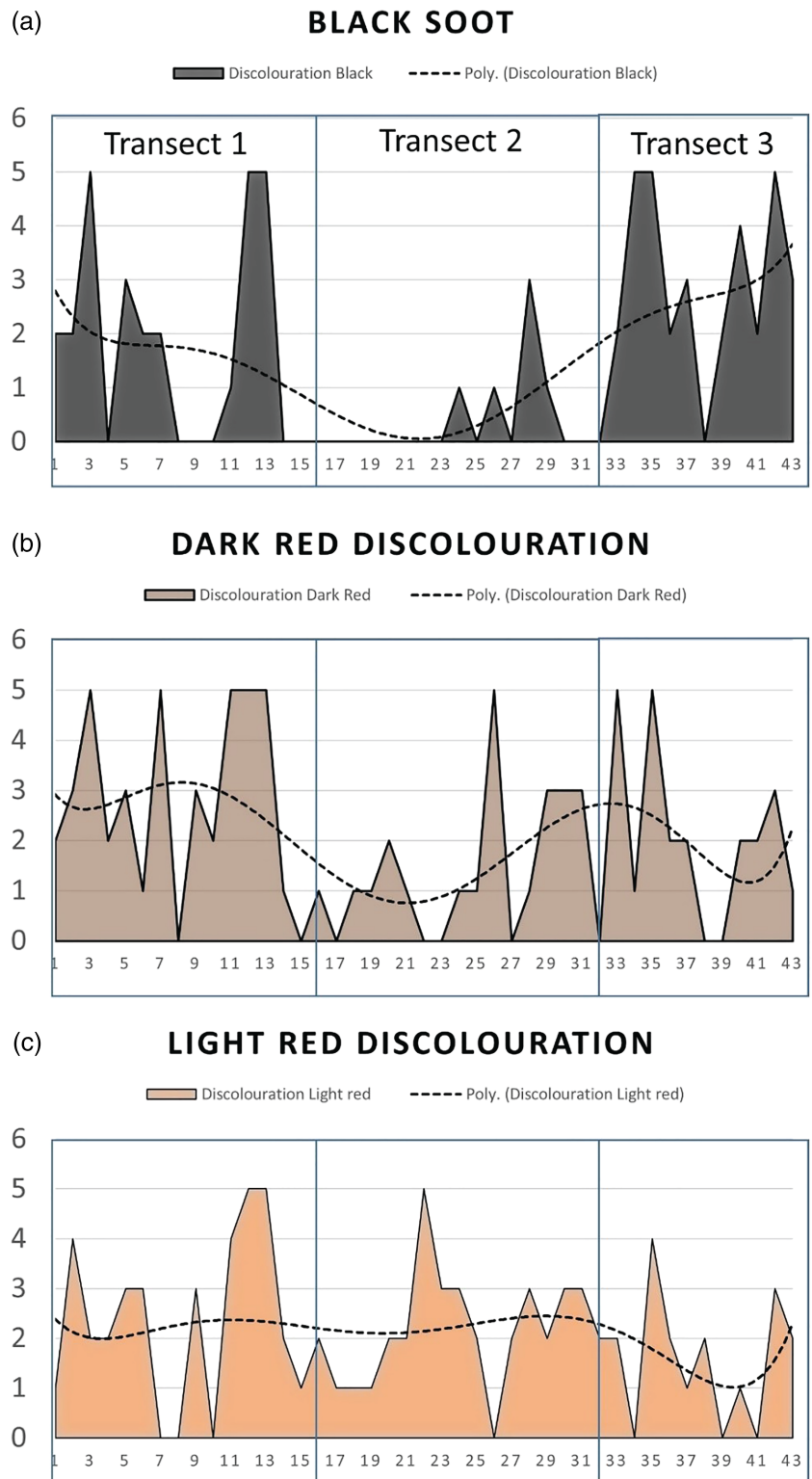


FIGURE 10 (a) Total damage recorded across all samples, plotted against sample size and (b) plotted by transect. The total damage score shows a poor correlation between sample rock size and damage score, but a much more noticeable correlation between total damage score and the placement of the sample rock within the landscape (i.e. the transect) [Color figure can be viewed at wileyonlinelibrary.com]

FIGURE 11 (a) Black soot deposition intensity observation scores; (b) dark red discolouration intensity observation scores; (c) light red discolouration intensity observation scores [Color figure can be viewed at wileyonlinelibrary.com]



indicative of some iron mobilization and oxidation (Gomez-Heras et al., 2009), does not show any clear relatively increased or decreased presence across transects 1 and 2, but is observed to a lesser degree at transect 3 (Figure 11c). This correlates with the observation that the most intense temperature increases are likely around the larger fuel sources along transect 3, and at the top of the slope, leading to higher temperatures and thus darker red discolouration.

4.6 | Crack formation (hypothesis 6)

The final hypothesis investigates the distribution of crack formation across all rock samples. As Figure 12 illustrates, crack formation showed some variation across the lithologies; both types of sandstone showed consistent evidence of macro-crack formation (Figure 12b), which was marginally less present in the Malmsbury Group sandstone rocks. Peninsula Formation sandstone appears most susceptible to

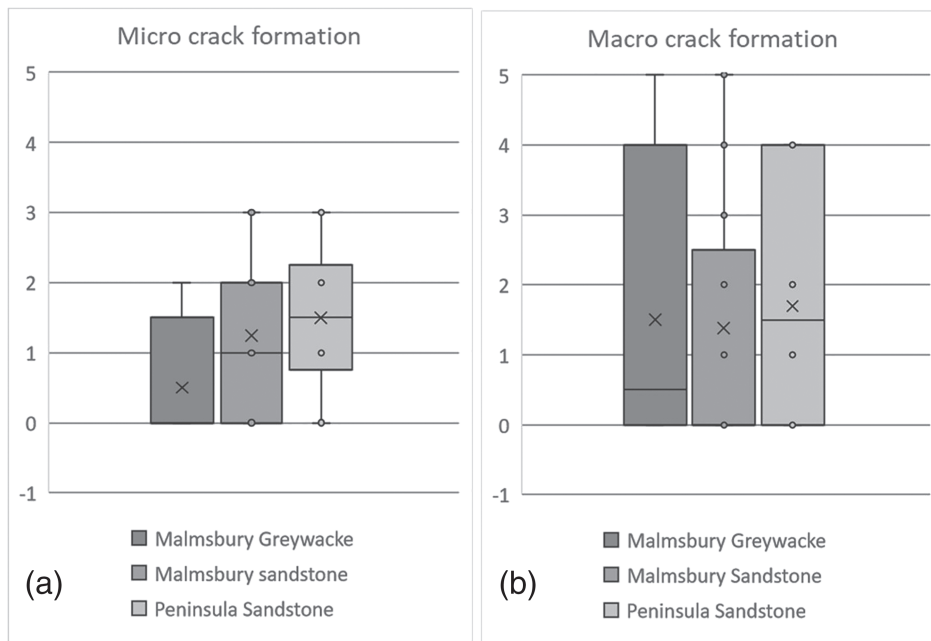


FIGURE 12 (a) Micro-crack (<1 mm width) formation as a function of lithology and (b) macro-crack (>1 mm) formation

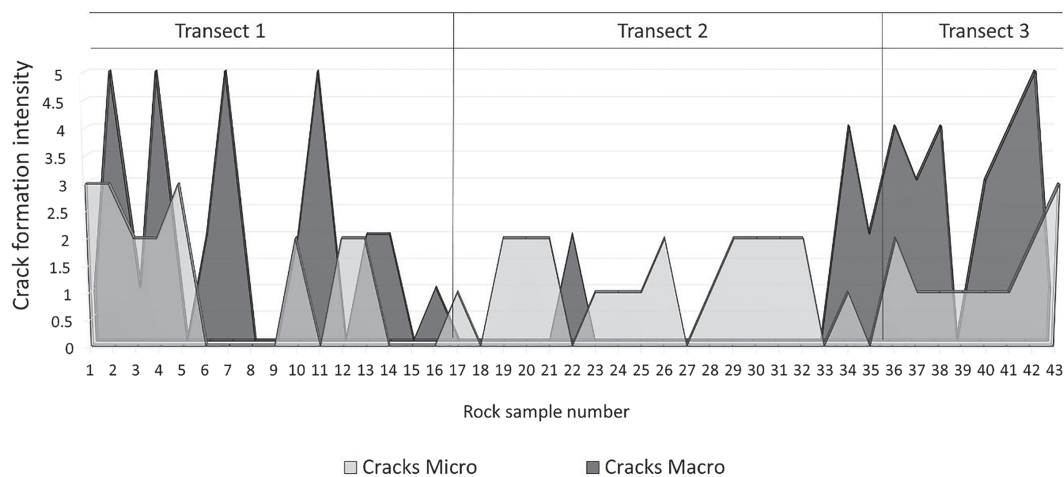


FIGURE 13 Micro- and macro-crack formation across all sample rocks, divided by transects

cracking, showing both the highest average micro-crack formation score (1.5) and macro-crack formation score (1.75). However, the Malmsbury Group greywacke and sandstone showed more varied results where the sandstone appears to sustain more micro-cracks, whereas greywacke appears more susceptible to macro-cracking.

As Figure 13 illustrates, micro-cracks (>1 mm width) are identified commonly throughout all samples. Macro-cracks (>1 mm width), in contrast, are only consistently observed at the top and bottom of the slope (transects 1 and 3).

5 | DISCUSSION

5.1 | The influence of topography on fire propagation and rock weathering

Based on the results presented in this study, the picture emerges of a more complex interplay between the topography and the pattern of fire damage observed on rock samples; the movement of both heat

and soot across the slope leaves behind a stepped signature of soot and heat alteration on the sampled rocks. In particular, soot deposition (Figure 11) and micro- and macro-crack formation (Figures 12 and 13) correspond well with the placement of the rock samples within the landscape. This opens up possibilities for fire intensity and direction reconstruction studies, as the damage can trace the fire's interaction with local variations in topography. The damage observed corresponds to previous studies conducted on wildfire-driven rock weathering (e.g. Dorn, 2003; Shtober-Zisu et al., 2018), but the propagation of the rising heat across even a small slope, such as the one studied here, brings in further nuance in the crack formation patterns observed. Extrapolating this observation into a function of wider landscape development after a wildfire, it could be hypothesized that where this pattern of differential weathering is repeated across a larger landscape, it is possible that long-term landscape alteration associated with weathering products is more heterogenous than previously assumed. This includes the contribution of rock fragments to surface cover, lowering erodibility within limited areas (e.g. transects 1 and 3, where spalling and large rock fragments were observed), but

equally leaving areas such as those along transect 2, where a comparatively reduced volume of weathering products was observed, more vulnerable to erosion.

5.2 | The influence of lithology and rock size on damage patterns

The initial results indicate that boulder size and lithology are of secondary importance to the placement of the affected rocks within the wider topography of the landscape. As Figure 10a shows, there is little direct correlation between sample size and the damage measured during the field survey. This does not preclude the production of spalls and other rock fragments, and their subsequent influence on soil cover and composition, as noted by Shtober-Zisu and Wittenberg (2021a). But it does indicate that the damage to rocks associated with wildfire can vary not just according to lithology and size, but foremost according to the placement of the rock within the landscape at the time of the fire.

5.3 | Wider topographical features and their effect on fire-driven damage to rocks

The presence of a water source at the bottom of the slope (Figures 2 and 14), and associated increase in moisture within the sampled rocks, is likely to exacerbate the response of the rocks to heat, such as the formation of macro-fractures. The TWI shown in Figure 2 indicates that the samples at transect 3 are exposed to higher moisture levels within the ground than those at transects 1 and 2. When assessing the impact of wildfire on rock weathering, the topography and thus fire intensity distributions therefore need to be considered. The analysis of the data indicated that in this case study there is no direct correlation between the type and severity of the outwardly visible damage sustained on the sampled rocks, and the size, lithology or proximity to burn source. This does not discredit the hypotheses set out in Table 1, but instead calls for a re-evaluation of fire-related damage in the wider context of rock response as a function of topographical variations.

5.4 | Topography-driven fire progression and its effect on damage patterns

When comparing the response of the sampled rocks to the fire across the transects, the most striking trend is the decreased observation of all damage indicators mid-way up the slope in transect 2. Utilizing work carried out on fire progression in domestic settings, this is likely connected to the development of a buoyant plume within the air column above the wildfire (Li et al., 2014; Ricks et al., 2010). At the bottom of the slope, the combination of a large fuel source in the form of the robust woody indigenous trees, fed by the moisture source and absorption of moisture by the sample rocks, produces both heat and steam that leads to the cracking of rocks. At the top of the buoyant plume, where the hot air disperses within the cooler air on top of the slope nearer transect 3, and the plume loses energy, there is marked deposition of soot (Xin & Gore, 2005). The middle of the slope (transect 2) does not experience the same sustained high temperatures, nor is it exposed to the moisture source as directly, and is largely passed over by the rising soot-laden plume, thus leading to reduced influence of wildfire on the rock samples. As shown in Figures 11, 12 and 13, there is by no means an absence of fire damage, as for example light red discolouration is observed on all transects, but factors such as soot deposition and macro-crack formation are observed in reduced intensities.

The semi-quantitative and quantitative research carried out in Jonkershoek therefore indicates that topography, including slope and moisture availability, are important factors in the effect that wildfire has on the deterioration of the investigated rocks. This concept is illustrated in Figure 14, showing the interaction between topography, the buoyant plume and the formation and deposition of soot on the rocks. This by no means precludes the other indicators of fire damage, such as discolouration and crack formation, as noted in previous studies, but indicates the importance of incorporating detail of the wider landscape setting in our approaches to understanding wildfire damage to rocks. By utilizing the insights of engineering fire studies, as cited throughout this research, we identify further patterns of wildfire damage.

These findings are particularly of interest when placed within the wider climate change context; the inherent alteration of the soil cover

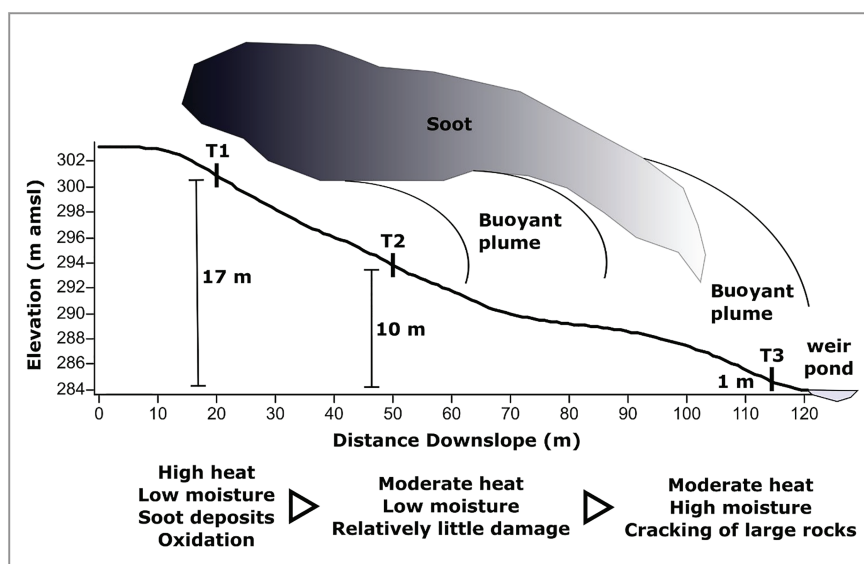


FIGURE 14 Conceptual model of topographically directed changes in fire behaviour on the investigated slope [Color figure can be viewed at [wileyonlinelibrary.com](https://onlinelibrary.wiley.com)]

could disrupt the recovery process of the soil, especially where wildfires are occurring more frequently than usual due to increasing drought cycles, alien vegetation invasion and anthropogenic ignition events (Kraaij & van Wilgen, 2014). The fires in 2015, which are investigated here, showed a distinct response of the measured rocks to the wildfire. If wildfire occurrence continues to increase in frequency, the associated increase in spalling and cracking of larger rocks could lead to increased soil cover with larger fragments, potentially altering the composition of the local vegetation, as well as more rapid surface sediment production as larger sandstone fragments disaggregate under subsequent wetting and drying. Thus, the combination of rock susceptibility to wildfire damage, as directed by the local topography, the changes in drought patterns and the invasion of alien woody vegetation in some cases (e.g. Mtengwana et al., 2021) could lead to altered catchment processes.

6 | CONCLUSIONS

Wildfires are an increasing risk in a climate that is becoming increasingly destabilized, whether increasing in frequency in areas where wildfires are relatively common—such as savannahs—or occurring in previously relatively unaffected areas such as the Arctic Circle. This research shows that while the damage observed on the rock samples corresponds to previous research, as the hypotheses derived from the wider literature are largely upheld by the findings presented here, further consideration needs to be given to the role of topography in fire development and progression. The differential zones within a fire interacting with a slope, as demonstrated in this research, lead to zoned deposition of soot and occurrence of structural damage such as cracking. Of the variables tested, the strongest statistical correlation found was the height of the transect placement on the slope as a determining factor of intensity of rock damage. Lithology and rock size were found to be less significant contributors to damage intensity at this field site. While the role of moisture in these processes warrants further research, the findings indicate that rock samples located in relatively wet zones are more prone to large-scale cracking. It is hoped that these findings motivate an approach to fire-driven rock weathering investigations that incorporates wider topography-driven analyses of the landscape setting and wildfire heat and ash-fall dynamics. By integrating the cited fire engineering studies, as well as wildfire topographical studies, into rock weathering analysis we can gain a greater understanding of the interplay between landscape, fire and the subsequent markings this leaves on the rocks subjected to the fire. This may yield further insights into the effect of wildfire on rock deterioration, and lead to further advances in understanding the role of fire in the interplay between landscapes and the earth surface processes that shape them.

ACKNOWLEDGEMENTS

The authors want to thank the British Society for Geomorphology for the Early Career Research Grant awarded to L. Mol that made this collaborative fieldwork possible. They also want to thank MTO Group for permission to work on site and The Bataleurs for their funding of the aerial investigation carried out by M. Grenfell. Finally, they want to thank two anonymous reviewers for their insightful and supportive comments.

DATA AVAILABILITY STATEMENT

All data can be provided by the authors upon request.

ORCID

Lisa Mol  <https://orcid.org/0000-0001-5272-3671>

Michael Grenfell  <https://orcid.org/0000-0001-8687-2181>

REFERENCES

- Abatzoglou, J.T. & Williams, A.P. (2016) Impact of anthropogenic climate change on wildfire across western US forests. *PNAS*, 113(42), 11770–11775. Available from: <https://doi.org/10.1073/pnas.1607171113>
- Allison, R.J. & Bristow, G.E. (1999) The effects of fire on rock weathering: Some further considerations of laboratory experimental simulation. *Earth Surface Processes and Landforms*, 24(8), 707–713. Available from: [https://doi.org/10.1002/\(SICI\)1096-9837\(199908\)24:8<707::AID-ESP993>3.0.CO;2-Z](https://doi.org/10.1002/(SICI)1096-9837(199908)24:8<707::AID-ESP993>3.0.CO;2-Z)
- Aoki, H. & Matsukura, Y. (2007) A new technique for non-destructive field measurement of rock-surface strength: An application of the Equotip hardness tester to weathering studies. *Earth Surface Processes and Landforms*, 32(12), 1759–1769. Available from: <https://doi.org/10.1002/esp.1492>
- Aponte, C., de Groot, W.J. & Wotton, B.M. (2016) Forest fires and climate change: Causes, consequences and management options. *Journal of the International Association of Wildland Fire*, 25(8), i–ii. Available from: https://doi.org/10.1071/WFv25n8_FO
- Beeson, P.C., Martens, S.N. & Breshears, D.D. (2001) Simulating overland flow following wildfire: Mapping vulnerability to landscape disturbance. *Hydrological Processes*, 15(15), 2971–2930. Available from: <https://doi.org/10.1002/hyp.382>
- Betts, M.W. & Latta, M.A. (2000) Rock surface hardness as an indication of exposure age: An archaeological application of the Schmidt Hammer. *Archaeometry*, 42(1), 209–223. Available from: <https://doi.org/10.1111/j.1475-4754.2000.tb00877.x>
- Bierman, P. & Gillespie, A. (1991) Range fires: A significant factor in exposure-age determination and geomorphic surface evolution. *Geology*, 19(6), 641–644. Available from: [https://doi.org/10.1130/0091-7613\(1991\)019<0641:RFASFI>2.3.CO;2](https://doi.org/10.1130/0091-7613(1991)019<0641:RFASFI>2.3.CO;2)
- Blackwelder, E. (1927) Fire as an agent in rock weathering. *Journal of Geology*, 35(2), 134–140. Available from: <https://doi.org/10.1086/623392>
- Boelhouwers, J. (1999) Relict periglacial slope deposits in the Hex River Mountains, Western Cape, South Africa. *Geomorphology*, 30(3), 245–258. Available from: [https://doi.org/10.1016/S0169-555X\(99\)00033-1](https://doi.org/10.1016/S0169-555X(99)00033-1)
- Boelhouwers, J. & Meiklejohn, K.I. (2002) Quaternary periglacial and glacial geomorphology of southern Africa: Review and synthesis. *South African Journal of Science*, 98, 47–55.
- Bormann, B.T., Homann, P.S., Darbyshire, R.L. & Morrisette, B.A. (2008) Intense forest wildfire sharply reduces mineral soil C and N: The first direct evidence. *Canadian Journal of Forest Research*, 38(11), 2771–2783. Available from: <https://doi.org/10.1139/X08-136>
- Bridge, S.R.J. & Johnson, E.A. (2009) Geomorphic principles of terrain organization and vegetation gradients. *Journal of Vegetation Science*, 11(1), 57–70.
- Buckman, S., Morris, R.H. & Bourman, R.P. (2021) Fire-induced rock spalling as a mechanism of weathering responsible for flared slope and inselberg development. *Nature Communications*, 12(1), 2150. Available from: <https://doi.org/10.1038/s41467-021-22451-2>
- Cerdà, A. (2001) Effects of rock fragment cover on soil infiltration, inter-rill runoff and erosion. *European Journal of Soil Science*, 52(1), 59–68. Available from: <https://doi.org/10.1046/j.1365-2389.2001.00354.x>
- Cerveney, N.V., Dorn, R.I., Allen, C.D. & Whitley, D.S. (2016) Advances in rapid condition assessments of rock art sites: Rock Art Stability Index (RASI). *Journal of Archaeological Science: Reports*, 10, 871–877.
- Collins, L., Penman, T.D., Price, O.F. & Bradstock, R.A. (2015) Adding fuel to the fire? Revegetation influences wildfire size and intensity.

- Journal of Environmental Management*, 150, 196–205. Available from: <https://doi.org/10.1016/j.jenvman.2014.11.009>
- Coombes, M.A., Feal-Pérez, A., Naylor, L.A. & Wilhelm, K. (2013) A non-destructive tool for detecting changes in the hardness of engineering materials: Application of the Equotip durometer in the coastal zone. *Engineering Geology*, 167, 14–19. Available from: <https://doi.org/10.1016/j.enggeo.2013.10.003>
- Costa, J.J., Oliveira, L.A., Viegas, D.X. & Neto, L.P. (1991) On the temperature distribution inside a tree under fire conditions. *International Journal of Wildland Fire*, 1(2), 87–96. Available from: <https://doi.org/10.1071/WF9910087>
- De Vente, J. & Poesen, J. (2005) Predicting soil erosion and sediment yield at the basin scale: Scale issues and semi-quantitative models. *Earth-Science Reviews*, 71(1–2), 95–125. Available from: <https://doi.org/10.1016/j.earscirev.2005.02.002>
- Deal, K. (2012) Fire effects on flaked stone, ground stone, and other stone artifacts. In: Ryan, K.C., Jones, A.T., Koerner, C.L. & Lee, K.M. (Eds.) *Wildland Fire in Ecosystems: Effects of Fire on Cultural Resources and Archaeology*. General Technical Report RMRS-GTR-42-vol. 3. Fort Collins, CO: U.S. Department of Agriculture, Forest Service, Rocky Mountain Research Station, pp. 97–111.
- Denny, M.W. (1993) *Air and Water: The Biology and Physics of Life's Media*. Princeton, NJ: Princeton University Press.
- Doerr, S.H., Shakesby, R.A., Blake, W.H., Chafer, C.J., Humphreys, G.S. & Wallbring, P.J. (2006) Effects of differing wildfire severities on soil wettability and implications for hydrological response. *Journal of Hydrology*, 319(1–4), 295–311. Available from: <https://doi.org/10.1016/j.jhydrol.2005.06.038>
- Dorn, R.I. (2003) Boulder weathering and erosion associated with a wildfire, Sierra Ancha Mountains, Arizona. *Geomorphology*, 55(1–4), 155–171. Available from: [https://doi.org/10.1016/S0169-555X\(03\)00138-7](https://doi.org/10.1016/S0169-555X(03)00138-7)
- Dorn, R.I., Dorn, J., Harrison, E., Gutbrod, E., Gibson, S., Larson, P., et al. (2012) Case hardening vignettes from the Western USA: Convergence form as a result of divergent hardening processes. *Yearbook of the Association of Pacific Coast Geographers*, 74(1), 53–75. Available from: <https://doi.org/10.1353/pcg.2012.0003>
- Dragovich, D. (1993) Fire-accelerated boulder weathering in the Pilbara, Western Australia. *Zeitschrift für Geomorphologie*, 37(3), 295–307. Available from: <https://doi.org/10.1127/zfg/37/1993/295>
- Emery, K.G. (1944) Brush fires and rock exfoliation. *American Journal of Science*, 242(9), 506–508. Available from: <https://doi.org/10.2475/ajs.242.9.506>
- Escuin, S., Navarro, R. & Fernández, P. (2008) Fire severity assessment by using NBR (Normalized Burn Ratio) and NDVI (Normalized Difference Vegetation Index) derived from LANDSAT TM/ETM images. *International Journal of Remote Sensing*, 29(4), 1053–1073. Available from: <https://doi.org/10.1080/01431160701281072>
- Fairman, T.A., Nitschke, C.R. & Bennett, L.T. (2015) Too much, too soon? A review of the effects of increasing wildfire frequency on tree mortality and regeneration in temperate eucalypt forests. *International Journal of Wildland Fire*, 25(8), 831–848.
- Geldenhuys, C.J. (1997) Native forest regeneration in pine and eucalypt plantations in Northern Province, South Africa. *Forest Ecology and Management*, 99(1–2), 101–115. Available from: [https://doi.org/10.1016/S0378-1127\(97\)00197-7](https://doi.org/10.1016/S0378-1127(97)00197-7)
- Gillhuber, S., Lehrberger, G. & Göske, J. (2010) Fire damage of trachyte: Investigations of the Teplá monastery building stones. *Geological Society of London, Special Publication*, 333(1), 73–79. Available from: <https://doi.org/10.1144/SP333.7>
- Gomez-Heras, M., McCabe, S., Smith, B.J. & Fort, R. (2009) Impacts of fire on stone-built heritage. *Journal of Architectural Conservation*, 15(2), 47–58. Available from: <https://doi.org/10.1080/13556207.2009.10785047>
- Goudie, A.S., Allison, R.J. & McLaren, S.J. (1992) The relations between modulus of elasticity and temperature in the context of the experimental simulation of rock weathering by fire. *Earth Surface Processes and Landforms*, 17(6), 605–615. Available from: <https://doi.org/10.1002/esp.3290170606>
- Gunn, R.G. (2011) The impact of bushfires and fuel reduction on the preservation of shelter rock art. *Rock Art Research*, 28(1), 53–70.
- Guo, T., Wang, Q., Li, D. & Zhuang, J. (2010) Effect of surface stone cover on sediment and solute transport on the slope of fallow land in the semi-arid loess region of northwestern China. *Journal of Soils and Sediments*, 10(6), 1200–1208. Available from: <https://doi.org/10.1007/s11368-010-0257-8>
- Haas, F., Heckmann, T., Wichmann, V. & Becht, M. (2012) Runout analysis of a large rockfall in the Dolomites/Italian Alps using LIDAR derived particle sizes and shapes. *Earth Surface Processes and Landforms*, 37(13), 1444–1455. Available from: <https://doi.org/10.1002/esp.3295>
- Hack, H.R.G.K., Hingira, J. & Verwaal, W. (1993) Determination of discontinuity wall strength by Equotip and ball rebound tests. *International Journal of Rock Mechanics and Mining Science and Geomechanics Abstracts*, 30(2), 151–155. Available from: [https://doi.org/10.1016/0148-9062\(93\)90707-K](https://doi.org/10.1016/0148-9062(93)90707-K)
- Hajpál, M. & Török, Á. (2004) Mineralogical and colour changes of quartz sandstones by heat. *Environmental Geology*, 46(3–4), 311–322.
- Hansen, C.D., Meiklejohn, K.I., Nel, W., Loubser, M.J. & Van Der Merwe, B.J. (2013) Aspect-controlled weathering observed on a blockfield in Dronning Maud Land, Antarctica. *Geografiska Annaler, Series A: Physical Geography*, 95(4), 305–313. Available from: <https://doi.org/10.1111/geoa.12025>
- Hu, L.H., Huo, R., Wang, H.B. & Yang, R.X. (2007) Experimental and numerical studies on longitudinal smoke temperature distribution upstream and downstream from the fire in a road tunnel. *Journal of Fire Sciences*, 25(1), 23–43. Available from: <https://doi.org/10.1177/0734904107062357>
- Jackson, M.A. (1998) *The nature of fire-cracked rock: New insights from ethnoarchaeological and laboratory experiments*. Master's thesis, Texas A&M University
- Janssens, M.L. (2004) Modeling of the thermal degradation of structural wood members exposed to fire. *Fire and Materials*, 28(2–4), 199–207. Available from: <https://doi.org/10.1002/fam.848>
- Jiang, Y., Rastetter, E.B., Shaver, G.R., Rocha, A.V., Zhuang, Q. & Kwiatkowski, B.L. (2016) Modeling long-term changes in tundra carbon balance following wildfire, climate change, and potential nutrient addition. *Ecological Applications*, 27(1), 105–117. Available from: <https://doi.org/10.1002/eap.1413>
- Jolly, W.M., Cochrane, M.A., Freeborn, P.H., Holden, Z.A., Brown, T.J., Williamson, G.J., et al. (2015) Climate-induced variations in global wildfire danger from 1979 to 2013. *Nature Communications*, 6, 7537. Available from: <https://doi.org/10.1038/ncomms8537>
- Jury, M.R. (2019) South Africa's future climate: Trends and projections. In: *The Geography of South Africa*. Cham: Springer, pp. 305–312.
- Kompaniková, Z., Gomez-Heras, M., Michňová, J., Durmeková, T. & Vlčko, J. (2014) Sandstone alterations triggered by fire-related temperatures. *Environmental Earth Sciences*, 72(7), 2569–2581. Available from: <https://doi.org/10.1007/s12665-014-3164-2>
- Kraaij, T. & van Wilgen, B.W. (2014) Drivers, ecology, and management of fire in fynbos. In: Allsop, N., Colville, J.F. & Verboom, G.A. (Eds.) *Fynbos: Ecology, Evolution, and Conservation of a Megadiverse Region*. Oxford: Oxford University Press, pp. 47–72.
- Lavee, H. & Poesen, J.W.A. (1991) Overland flow generation and continuity on stone-covered soil surfaces. *Hydrological Processes*, 5(4), 345–360. Available from: <https://doi.org/10.1002/hyp.3360050403>
- Leh, M.D., Murdoch, C.J., Brahana, J.V. & Haggard, B.E. (2008) Delineating runoff processes and critical runoff source areas in a pasture hillslope of the Ozark Highlands. *Hydrological Processes*, 22(21), 4190–4204. Available from: <https://doi.org/10.1002/hyp.7021>
- Li, L., Cheng, X., Wang, X. & Zhang, H. (2012) Temperature distribution of fire-induced flow along tunnels under natural ventilation. *Journal of Fire Sciences*, 30(2), 122–137. Available from: <https://doi.org/10.1177/0734904111428896>
- Li, L.J., Fan, C.G., Sun, J.H., Yuan, X.Y. & Shi, W.X. (2014) Experimental investigation on the characteristics of buoyant plume movement in a stairwell with multiple openings. *Energy and Buildings*, 68(Part A),

- 108–120. Available from: <https://doi.org/10.1016/j.enbuild.2013.09.028>
- Li, X.-Y. & Liu, L.-Y. (2003) Effect of gravel mulch on Aeolian dust accumulation in the semiarid region of northwest China. *Soil and Tillage Research*, 70(1), 73–81. Available from: [https://doi.org/10.1016/S0167-1987\(02\)00137-X](https://doi.org/10.1016/S0167-1987(02)00137-X)
- Malkinson, D. (2012) Wildfire heterogeneity: Empirical vs. simulated observations – the Carmel 2010 wildfire as a case study. *Israel Journal of Ecology & Evolution*, 58(2–3), 165–176.
- Maswanganye, S.E. (2017) *A comparison of remotely-sensed precipitation estimates with observed data from rain gauges in the Western Cape, South Africa*. Unpublished MSc Thesis, University of the Western Cape, South Africa.
- McCabe, S., Smith, B.J. & Warke, P.A. (2007) Sandstone response to salt weathering following simulated fire damage: A comparison of the effects of furnace heating and fire. *Earth Surface Processes and Landforms*, 32(12), 1874–1883. Available from: <https://doi.org/10.1002/esp.1503>
- McCarroll, D. (1991) The Schmidt hammer, weathering and rock surface roughness. *Earth Surface Processes and Landforms*, 16(5), 477–480. Available from: <https://doi.org/10.1002/esp.3290160510>
- Mol, L. & Viles, H.A. (2012) The role of rock surface hardness and internal moisture in tafoni development in sandstone. *Earth Surface Processes and Landforms*, 37(3), 301–314. Available from: <https://doi.org/10.1002/esp.2252>
- Moody, J.A. & Martin, D.A. (2001) Initial hydrologic and geomorphic response following a wildfire in the Colorado Front Range. *Earth Surface Processes and Landforms*, 26(10), 1049–1070. Available from: <https://doi.org/10.1002/esp.253>
- Moon, B.P. (1991) The forms of rock slopes in the Cape Fold Mountains. *South African Geographical Journal*, 66(1), 16–31. Available from: <https://doi.org/10.1080/03736245.1984.10559686>
- Mordandini, F., Santoni, P.A. & Balbi, J.H. (2001) The contribution of radiant heat transfer to laboratory-scale fire spread under the influences of wind and slope. *Fire Safety Journal*, 36(6), 519–543. Available from: [https://doi.org/10.1016/S0379-7112\(00\)00064-3](https://doi.org/10.1016/S0379-7112(00)00064-3)
- Moses, G. (2008) *The establishment of long-term rainfall trends in the annual rainfall patterns in the Jonkershoek valley, Western Cape, South Africa*. Unpublished MSc Thesis, University of the Western Cape, South Africa.
- Mtengwana, B., Dube, T., Mudereri, B.T. & Shoko, C. (2021) Modeling the geographic spread and proliferation of invasive alien plants (IAPs) into new ecosystems using multi-source data and multiple predictive models in the Heuningnes catchment, South Africa. *GIScience & Remote Sensing*, 58(4), 483–500. Available from: <https://doi.org/10.1080/15481603.2021.1903281>
- Neave, M. & Rayburg, S. (2007) A field investigation into the effects of progressive rainfall-induced soil seal and crust development on runoff and erosion rates: The impact of surface cover. *Geomorphology*, 87(4), 378–390. Available from: <https://doi.org/10.1016/j.geomorph.2006.10.007>
- Obaidullah, M., Bram, S., Verma, V.K. & De Ruyck, J. (2012) A review on particle emissions from small scale biomass combustion. *International Journal of Renewable Energy Research*, 2(1), 147–159.
- Ollier, C.D. (1983) Fire and rock breakdown. *Zeitschrift für Geomorphologie*, 27(3), 363–374. Available from: <https://doi.org/10.1127/zfg/27/1983/363>
- Pérez Alberti, A., Gomes, A., Trenhaile, A., Oliveira, M. & Horacio, J. (2013) Correlating river terrace remnants using an Equotip hardness tester: An example from the Miño River, northwestern Iberian Peninsula. *Geomorphology*, 192, 59–70. Available from: <https://doi.org/10.1016/j.geomorph.2013.03.017>
- Pierson, F.B., Robichaud, P.R. & Spaeth, K.E. (2001) Spatial and temporal effects of wildfire on the hydrology of a steep rangeland watershed. *Hydrological Processes*, 15(15), 2905–2916. Available from: <https://doi.org/10.1002/hyp.381>
- Potvin, D.A., Paris, K.M., Smith Date, K.L., Keely, C.C., Bray, R.D., Hale, J., et al. (2016) Genetic erosion and escalating extinction risk in frogs with increasing wildfire frequency. *Journal of Applied Ecology*, 54(3), 945–954.
- Pozo-Antonio, J.S., Sanmartín, P., Serrano, M., De la Rosa, J.M., Miller, A. Z. & Sanjurjo-Sánchez, J. (2020) Impact of wildfire on granite outcrops in archaeological sites surrounded by different types of vegetation. *Science of the Total Environment*, 747, 141143. Available from: <https://doi.org/10.1016/j.scitotenv.2020.141143>
- Rebello, A.G., Boucher, C., Helme, N., Mucina, L. & Rutherford, M.C. (2006) Fynbos biome. In: Mucina, L. & Rutherford, M.C. (Eds.) *The Vegetation of South Africa, Lesotho and Swaziland*. Pretoria: South African National Biodiversity Institute, pp. 53–219.
- Ricks, A.J., Hewson, J.C., Kerstein, A.R., Gore, J.P., Tieszen, S.R. & Ashurst, W.T. (2010) Spatially developing one-dimensional turbulence (ODT) study of soot and enthalpy evolution in meter-scale buoyant turbulent flames. *Combustion Science and Technology*, 182(1), 60–101. Available from: <https://doi.org/10.1080/00102200903297003>
- Rodríguez-Rellán, C. (2016) Variability of the rebound hardness as a proxy for detecting the levels of continuity and isotropy in archaeological quartz. *Quaternary International*, 424, 191–211. Available from: <https://doi.org/10.1016/j.quaint.2015.12.085>
- Roth, E.S. (1975) Temperature and water content as factors in desert weathering. *Journal of Geology*, 73(3), 454–468. Available from: <https://doi.org/10.1086/627077>
- Rulli, M.C. & Rosso, R. (2007) Hydrologic response of upland catchments to wildfires. *Advances in Water Resources*, 30(10), 2072–2086. Available from: <https://doi.org/10.1016/j.advwatres.2006.10.012>
- Sass, O., Haas, F., Schimmer, C., Heel, M., Bremer, M., Stöger, F. & Wetzel, K.-F. (2012) Impact of forest fires on geomorphic processes in the Tyrolean limestone alps. *Geografiska Annaler, Series A: Physical Geography*, 94(1), 117–133. Available from: <https://doi.org/10.1111/j.1468-0459.2012.00452.x>
- Scott, D.F. (1993) The hydrological effects of fire in South African mountain catchments. *Journal of Hydrology*, 150(2–4), 409–432. Available from: [https://doi.org/10.1016/0022-1694\(93\)90119-T](https://doi.org/10.1016/0022-1694(93)90119-T)
- Shakesby, R.A., Coelho, C.D.A., Feirreira, A.D., Terry, J.P. & Walsh, R.P.D. (1993) Wildfire impacts on soil-erosion and hydrology in wet Mediterranean forest, Portugal. *International Journal of Wildland Fire*, 3(2), 95–110. Available from: <https://doi.org/10.1071/WF9930095>
- Sharples, J.J. (2008) Review of formal methodologies for wind-slope correction on wildfire rate of spread. *International Journal of Wildland Fire*, 17(2), 179–193. Available from: <https://doi.org/10.1071/WF06156>
- Sharples, J.J. (2009) An overview of mountain meteorological effects relevant to fire behaviour and bushfire risk. *International Journal of Wildland Fire*, 18(7), 737–754. Available from: <https://doi.org/10.1071/WF08041>
- Shtober-Zisu, N., Brook, A., Kopel, D., Roberts, D., Ichoku, C. & Wittenberg, L. (2018) Fire induced rock spalls as long-term traps for ash. *Catena*, 162, 88–99. Available from: <https://doi.org/10.1016/j.catena.2017.11.021>
- Shtober-Zisu, N. & Wittenberg, L. (2021a) Long-term effects of wildfire on rock weathering and soil stoniness in the Mediterranean landscapes. *Science of the Total Environment*, 762, 143125. Available from: <https://doi.org/10.1016/j.scitotenv.2020.143125>
- Shtober-Zisu, N. & Wittenberg, L. (2021b) Wildfires as a weathering agent of carbonate rocks. *Minerals*, 11(10), 1091. Available from: <https://doi.org/10.3390/min11101091>
- Sian, K.T.C.L.K., Wang, J., Ayugi, B.O., Nooni, I.K. & Ongoma, V. (2021) Multi-decadal variability and future changes in precipitation over Southern Africa. *Atmosphere*, 12(6), 742. Available from: <https://doi.org/10.3390/atmos12060742>
- Sippel, J., Sigismund, S., Weiss, T., Nitsch, K.-H. & Korzen, M. (2007) Decay of natural stones caused by fire damage. *Geological Society of London, Special Publication*, 271(1), 139–151. Available from: <https://doi.org/10.1144/GSL.SP.2007.271.01.15>
- Smith, H.G., Sheridan, G.J., Lane, P.N.J., Noske, P.J. & Heijnis, H. (2011) Changes to sediment sources following wildfire in a forested upland catchment, Southeastern Australia. *Hydrological Processes*, 25(18), 2878–2889. Available from: <https://doi.org/10.1002/hyp.8050>
- Solly, M. (2019) *The Arctic is experiencing its worst wildfire season on record*. Washington DC, USA: Smithsonian Institution, Available from:

- <https://www.smithsonianmag.com/smart-news/arctic-experiencing-its-worst-wildfire-season-record-180972749/> [accessed 4/11/2019].
- Steel, Z.L., Safford, H.D. & Viers, J.H. (2015) The fire frequency–severity relationship and the legacy of fire suppression in California forests. *Ecosphere*, 6(1), 1–23. Available from: <https://doi.org/10.1890/ES14-00224.1>
- Stevens-Rumann, C.S., Kemp, K.B., Higuera, P.E., Harvey, B.J., Rother, M.T., Donato, D.C., et al. (2018) Evidence for declining forest resilience to wildfires under climate change. *Ecology Letters*, 21(2), 243–252. Available from: <https://doi.org/10.1111/ele.12889>
- Sullivan, A.L. (2017) Inside the inferno: Fundamental processes of wildland fire behaviour. Part 2: Heat transfer and interactions. *Current Forestry Reports*, 3(2), 150–171. Available from: <https://doi.org/10.1007/s40725-017-0058-z>
- Sullivan, A.L., McCaw, W.L., Cruz, M.G., Matthews, S. & Ellis, P.F. (2017) Fuel, fire weather and fire behaviour in Australian ecosystems. In: Williams, R.J., Gill, M.A. & Bradstock, R.A. (Eds.) *Flammable Australia: Fire Regimes, Biodiversity and Ecosystems in a Changing World*. Collingwood: CSIRO Publishing, pp. 51–78.
- Tarboton, D.G. (1997) A new method for the determination of flow directions and contributing areas in grid digital elevation models. *Water Resources Research*, 33(2), 309–319. Available from: <https://doi.org/10.1029/96WR03137>
- Tratebas, A.M., Cervený, N.V. & Dorn, R.I. (2004) The effects of fire on rock art: Microscopic evidence reveals the importance of weathering rinds. *Physical Geography*, 25(4), 313–333. Available from: <https://doi.org/10.2747/0272-3646.25.4.313>
- Verwaal, W. & Mulder, A. (1993) Estimating rock strength with the Equotip hardness tester. *International Journal of Rock Mechanics and Mining Science and Geomechanics Abstracts*, 30(6), 659–662. Available from: [https://doi.org/10.1016/0148-9062\(93\)91226-9](https://doi.org/10.1016/0148-9062(93)91226-9)
- Viles, H., Goudie, A., Grab, S. & Lalley, J. (2011) The use of the Schmidt Hammer and Equotip for rock hardness assessment in geomorphology and heritage science: A comparative analysis. *Earth Surface Processes and Landforms*, 36(3), 320–333. Available from: <https://doi.org/10.1002/esp.2040>
- Weise, D.R. & Biging, G.S. (1997) A qualitative comparison of fire spread models incorporating wind and slope effects. *Forest Science*, 43(2), 170–180.
- Wigtil, G., Hammer, R.B., Kline, J.D., Mockrin, M.H., Stewart, S.I., Roper, D., et al. (2016) Places where wildfire potential and social vulnerability coincide in the coterminous United States. *International Journal of Wildland Fire*, 25(8), 896–908. Available from: <https://doi.org/10.1071/WF15109>
- van Wilgen, B.W., Forsyth, G.G., De Klerk, H., Das, S., Khuluse, S. & Schmitz, P. (2010) Fire management in Mediterranean-climate shrublands: A case study from the Cape fynbos, South Africa. *Journal of Applied Ecology*, 47(3), 631–638. Available from: <https://doi.org/10.1111/j.1365-2664.2010.01800.x>
- Wilhelm, K., Viles, H. & Burke, Ó. (2016) Low impact surface hardness testing (Equotip) on porous surfaces – advances in methodology with implications for rock weathering and stone deterioration research. *Earth Surface Processes and Landforms*, 41(8), 1027–1038. Available from: <https://doi.org/10.1002/esp.3882>
- Wotton, B.M., Flannigan, M.D. & Marshall, G.A. (2017) Potential climate change impacts on fire intensity and key wildfire suppression thresholds in Canada. *Environmental Research Letters*, 12(9), 095003. Available from: <https://doi.org/10.1088/1748-9326/aa7e6e>
- Xin, Y. & Gore, J.P. (2005) Two-dimensional soot distributions in buoyant turbulent fires. *Proceedings of the Combustion Institute*, 30(1), 719–726. Available from: <https://doi.org/10.1016/j.proci.2004.08.126>
- Yue, X., Mickley, L.J., Logan, J.A., Hudman, R.C., Martin, M.V. & Yantosca, R.M. (2015) Impact of 2050 climate change on North American wildfire: Consequences for ozone air quality. *Atmospheric Chemistry and Physics*, 15(17), 10033–10055. Available from: <https://doi.org/10.5194/acp-15-10033-2015>
- Zang, C. & Li, G.-Q. (2017) Response of steel members subject to temperature gradient in localised fires. In: Harada, K., Matsuyama, K., Himoto, K., Nakamura, Y. & Wakatsuki, K. (Eds.) *Fire Science and Technology 2015*. Singapore: Springer, pp. 309–317.
- Zhao, C., Zhang, H., Wang, M., Jiang, H., Peng, J. & Wang, Y. (2021) Impacts of climate change on wind erosion in Southern Africa between 1991 and 2015. *Land Degradation & Development*, 32(6), 2169–2182. Available from: <https://doi.org/10.1002/ldr.3895>
- Zhou, X., Mahalingam, S. & Weise, D. (2007) Experimental study and large eddy simulation of effect of terrain slope on marginal burning in shrub fuel beds. *Proceedings of the Combustion Institute*, 31(2), 2547–2555. Available from: <https://doi.org/10.1016/j.proci.2006.07.222>

How to cite this article: Mol, L. & Grenfell, M. (2022) Influence of landscape moisture sources and topography on rock weathering patterns associated with wildfire. *Earth Surface Processes and Landforms*, 47(7), 1761–1777. Available from: <https://doi.org/10.1002/esp.5345>